Highly nonlinear and dispersion flattened fiber design for ultrafast phase sensitive amplification

H. Tilanka Munasinghe, Shahraam Afshar V., & Tanya M. Monro

***Abstract*—The properties of phase sensitive amplification (PSA) in highly nonlinear fibers are studied. We present a soft glass fiber designed for high nonlinearity and broadband, low dispersion and simulate its performance as a PSA device for ultrafast bitrate signals at 640 Gb/s. The effect of the fiber design parameters on its PSA performance have been studied and the final design has been optimised using a genetic algorithm to have a high nonlinearity and low, flat dispersion. This design has subsequently been compared to other highly nonlinear fibers in order to highlight the effect of both using soft glass and the design and optimisation technique. Modelled fiber performance shows squeezing of phase noise in a 5 m length of fiber with 32 dBm total power in the signal and pumps. The fiber length we have used in our model is two orders of magnitude shorter than the state of the art silica based PSA devices for comparable power levels. In addition, fabrication tolerance modelling is done to show that our fiber design is better able to manage fluctuations in the dispersion due to the high nonlinearity.**

***Index Terms*—Nonlinear fiber optics, soft glass, microstructured optical fiber, four wave mixing, phase sensitive amplification, broad band telecommunication networks, optical communication.**

I. Introduction

PHASE sensitive amplification is a parametric amplification process that has long been known in quantum mechanics as a mechanism for producing so-called 'squeezed states' of light [1], [2]. In the classical regime phase sensitive amplification has potential for all optical noise reduction and this has recently attracted considerable interest due to its numerous optical signal processing applications [3-6].

One application of particular interest is the reduction in phase noise introduced during transmission of phase modulated signal formats such as differential phase shift keying (DPSK). Such phase-keyed formats are generally considered more robust and offer many advantages compared to traditional on-off keyed (OOK) formats including extended transmission distance and enhanced line capacity [3], [4]. In addition to facilitating the use of DPSK type formats phase sensitive amplifiers can also, in principle, operate with a theoretical noise figure of 0 dB - as opposed to phase insensitive counterparts such as Erbium Doped fiber Amplifiers (EDFAs) which have a quantum noise limit of 3 dB [5], [6]. Recent work has, in fact, experimentally demonstrated a phase sensitive amplifier with a record low 1.1 dB noise figure [7].

In fiber optic systems phase sensitive amplification can be realised either through the use of a nonlinear optical loop mirror (NOLM) [8], [9] or via four wave mixing [14-16] . While both have successfully been demonstrated, the four wave mixing approach is advantageous as it offers the possibility of using multiple channels and therefore supports wavelength division multiplexing (WDM) type applications. But experimental realisation of phase sensitive amplifiers using four wave mixing has been difficult due to the need to maintain a fixed phase relationship between the signal and the pumps at the input [10].

However, recent work [11] has shown that this can be overcome by generating the pump waves from part of the signal before amplifying it in a two-stage process. This 'black box' configuration automatically locks the phase of the pump and signal waves and offers a pragmatic approach to processing real world signals.

While the experimental configuration is an important practical consideration, the nonlinear medium in which the parametric process occurs is crucial to the efficient functionality of the device. To date, dispersion shifted silica based Highly Nonlinear fibers (HNLFs) with nonlinearities in the order of 10 $W^{-1}km^{-1}$ are the standard in fiber based systems. The low loss and robustness of these fibers make them attractive for such telecoms applications but their low nonlinearity, relative to soft glass fibers, render the operating length of fiber to be a few hundred metres.

This paper explores the premise that switching to soft glass microstructured fibers enables one to access a regime where the gain, per length, is both higher and, by design, can be prevalent over a broad band. This allows us to potentially fabricate devices with fiber lengths in the order of meters, compared to the hundreds of metres that are generally required when using silica based HNLFs. For some applications there may also be a significant reduction in the required optical power, to sub Watt levels. A broad operation bandwidth is also important for the management of telecommunication networks as they move into the next generation, where high signal bitrates approaching 1 Tb/s and beyond become more common [12].

We present a fiber design that could potentially work in a dual pump scheme to squeeze phase noise in an ultrafast signal at 640 Gb/s. Phase sensitive amplification at such speeds has hitherto not been demonstrated, either experimentally or numerically - it is roughly 16 times faster than the highest bit rates that have been investigated. A consequence of the high bit rate of the signal is it requires that the fiber design to be able to operate over a broad bandwidth. The fiber we have designed is based on soft glass and has been designed to provide nonlinearity ($\gamma = 1099$ $W^{-1}km^{-1}$ at 1550nm) orders of magnitude greater than silica based HNLF and has its dispersion tailored to be low across the telecoms wavelengths with the zero dispersion at 1550 nm.

The fiber design was developed in terms of a set of geometric parameters that could be fed into a genetic algorithm in order to optimise its critical properties, namely the nonlinearity and dispersion. The individual effect of these parameters on the fiber properties has been shown in order to emphasise the need to use an optimisation technique such as a genetic algorithm for such complex fiber designs.

The performance of the fiber was then evaluated numerically, showing that we are able to squeeze phase noise in a 640 Gb/s signal stream without a significant penalty in terms of amplitude noise. Additionally, we are able to demonstrate this with a relatively short fiber length and total power (pumps and the signal) of 32 dBm. The total power is comparable to the state of the art in silica based PSA devices, however the fiber length is two orders of magnitude shorter. We have also modelled the effect of structural deviations that may occur during fabrication on the PSA performance. This modelling shows that, due to the optimised dispersion and high nonlinearity of the fiber, we are able to tolerate reasonably expected deviations in the dispersion profile of the fiber quite well.

II. Theory of phase sensitive amplification

In this paper we consider the case of two pump degenerate four wave mixing (FWM), where the frequency condition $2\omega_{s,i} = \omega_{P1} + \omega_{P2}$ is satisfied, i.e. where the signal and idler are degenerate and lie between the pumps. The signal, idler and pump waves are also assumed to be coplanar. A theoretical description of this scenario, along with some others, is well covered in [13]. The same formalism is adopted here.

A_{P1} and A_{P2} represent the field amplitudes at the pump wavelengths and $A_{s,i}$ is the field at the degenerate signal/idler wavelengths. The fiber nonlinearity is represented by the nonlinear coefficient γ and $\Delta\beta$ is the phase mismatch, defined below in Eq. (5). After propagation the final output $A_{s,i}$ can be written as below, in terms of the transformed signal amplitude $B_{s,i}$ and transfer functions μ and ν.

$$A_{s,i}(z) = B_{s,i}(z)\exp[-i\Delta\beta z/2 + i3\gamma(P_{P2}+P_{P1})z/2] \quad (1)$$

$$B_{s,i}(z) = \mu(z)B_{s,i}(0) + \nu(z)B^*_{s,i}(0) \quad (2)$$

$$\mu = \cosh(gz) - i\frac{\kappa}{2g}\sinh(gz) \quad (3)$$

$$\nu = i\frac{2\gamma A_{P1}(0)A_{P2}(0)}{g}\sinh(gz) \quad (4)$$

The input pump fields are given by $A_{P1}(0)$ and $A_{P2}(0)$ and we have used the quantities $\Delta\beta$, κ, and g for the phase mismatch, phase matching factor and parametric gain, respectively. They are defined below, where $\beta_{s,i}$ is the propagation constant at the signal/idler wavelength, while β_{P1}, β_{P2} are those for the two pumps. The pump powers are denoted by P_{P1} and P_{P2}, where $P_{Pi} = |A_{Pi}|^2 (i = 1, 2)$.

$$\Delta\beta = 2\beta_{s,i} - \beta_{P1} - \beta_{P2} \quad (5)$$

$$\kappa = \Delta\beta + \gamma(P_{P1} + P_{P2}) \quad (6)$$

$$g = \left(4\gamma^2 P_{P1}P_{P2} - \frac{\kappa^2}{2}\right)^{1/2} \quad (7)$$

Note that given Eq. (7), the transfer functions satisfy the condition $|\mu|^2 - |\nu|^2 = 1$. The phase dependant nature of the gain can be easily seen by considering the simple case where the phase is perfectly matched such that $\kappa = 0$. In this case we can write

$$\begin{aligned} B_{s,i}(z) &= \cosh(gz)B_{s,i}(0) + i\sinh(gz)B^*_{s,i}(0) \quad (8)\\ &= \frac{e^{gz}+e^{-gz}}{2}B_{s,i}(0) + i\frac{e^{gz}-e^{-gz}}{2}B^*_{s,i}(0)\\ &= e^{gz}\frac{B_{s,i}(0)+iB^*_{s,i}(0)}{2} + e^{-gz}\frac{B_{s,i}(0)-iB^*_{s,i}(0)}{2} \end{aligned}$$

Showing that the signal quadrature $\frac{1}{2}[B_{s,i}(0) + iB^*_{s,i}(0)]$ is amplified by the factor e^{gz} while the $\frac{1}{2}[B_{s,i}(0) - iB^*_{s,i}(0)]$ quadrature is attenuated by the same factor. Thus the phase sensitive gain, given by the ratio of the amplified factor to the attenuated one is given by $G_{PSA} = e^{2gz}$.

This analytical description illustrates the nature of phase sensitive amplification for the two-pump scheme. The gain factor, g, presented in this analysis (see Eq. (7)) is crucial in determining how well a fiber may work as a PSA device and is therefore used in the optimisation procedure of the fiber design. However it should be noted that the above analysis is only valid in the small signal regime where the pumps are not depleted. Hence, in this paper pulse propagation is performed numerically to evaluate the PSA performance without the need for the small signal approximation. This allows us to, for instance, evaluate PSA performance in the saturated regime where the pumps are depleted.

III. Fiber design

We see from Eq. (5) to (7) that the gain for the nonlinear four wave mixing process is largely determined by wavelength dependance of the propagation constant. Mainly because this, in turn, determines the amount of phase mismatch, $\Delta\beta$ between the signal/idler and pump waves. Additionally, as we see from Eq. (6) and (7), the nonlinearity of the fiber is also important. Given that $\gamma(P_{P1} + P_{P2})$ is a slow function of λ, low dispersion slope is an important design consideration for efficient device functionality, along with a high nonlinear coefficient.

For the initial fiber design we considered a high index soft glass material for high nonlinearity. The choice of soft glass is important for two reasons. The first being the access to high intrinsic material nonlinearity, as is typical for high index glasses, in accordance with Miller's rule [14] (which states that the nonlinear refractive index is approximately proportional to the linear refractive index). The second is the relatively low softening point (typically a few hundred degrees) that allows extrusion into complex structures, such as the hexagonal structure shown in Fig. 1.

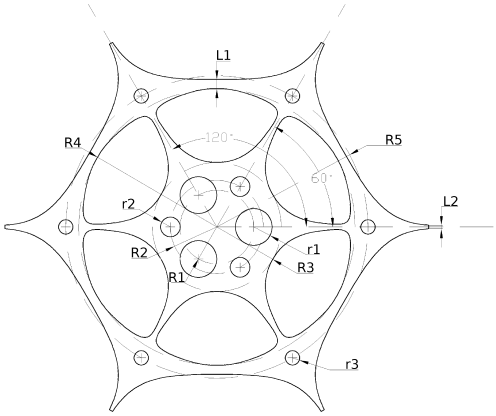

Fig. 1: Initial fiber geometry used in the genetic algorithm. The fiber parameters shown above were used to optimise the design for low dispersion and high nonlinearity

The specific material chosen for the fiber design was one of the Asahi bismuth-oxide glasses, BIAB061. This glass is well suited for the fabrication of highly nonlinear fibers due to its high nonlinear index, n_2, of 3.2×10^{-19} m^2W^{-1} [15], an order of magnitude higher that that for fused silica [16]. In addition, the glass is also known to have good mechanical and thermal stability which aids the fabrication process. Bismuth oxide glasses have been used extensively for the fabrication of high quality microstructured optical fibers [17], [18]

The geometry of our initial fiber design is a hybrid hexagonal/suspended core design type structure for dispersion engineering. We call this structure a 'hexagonal wagon wheel' (HWW). The HWW geometry is based on previous work [19] which focused on designing dispersion engineered fibers for supercontinuum generation in the mid infrared [20]. It consists of a suspended core containing a ring of holes, as shown in Fig. 1. The size and placement of the holes in the core region enables control of the waveguide dispersion while the suspended core provides high confinement. The latter both minimises confinement loss and increases the nonlinearity. Note that the geometry shown in Fig. 1 contains only the core region of the fiber. Since we used a Finite Element Method (FEM) model to calculate the dispersion and nonlinearity of the fiber, including the cladding region would only have added to the computation time without providing any additional useful information.

As in [20], [21] we optimise this structure by first parameterising it in terms of R1, R2, R3, R4, R5, r1, r2, r3, L1 and L2. Of those parameters, the ones that determine the dispersive and nonlinear properties of the fiber are R1, R2, R3, R4 r1 and r2 - the rest effectively serve to hold the structure together and have no effect on the guidance of the fiber.

The parameters r1 and R1 are used to describe a circular ring of three holes around the centre of the fiber - r1 is the radius of these holes and R1 is the distance between the centers of these holes and the centre of the fiber. Similarly, r2 and R2 describe a second ring of holes, interleaved with the first. In general, to achieve fine dispersion control, we must consider independently varying r1, r2, R1 and R2 i.e., two sets of inner holes, each with a different radius and distance away from the centre. However, such a design presents significant fabrication challenges. Therefore, in the interests of designing a fiber that is within reasonable fabrication limits we have set r1 = r2 and R1 = R2. The parameters R3 and R4 largely determine the radius of the suspended core region. They affect the confinement of the mode and, in turn, the dispersion and the nonlinearity of the fiber.

While each individual parameter has an effect on the guidance of the mode within the fiber, it is the complex interplay between them that determines the final fiber properties. Therefore, even though it may be possible to infer trends for individual parameters, the effect of varying multiple parameters simultaneously is difficult to ascertain and predict with any confidence, without performing extensive simulations. Thus the need for a genetic algorithm type optimisation procedure. The final values obtained through this optimisation procedure are shown in Table I.

TABLE I: Optimal parameter set

Parameter(s)	Value
r1, r2	120 nm
R1, R2	619 nm
R3	810 nm
R4	1.66 μm

In Fig. 2. below we show the effect of varying each parameter (about the ideal, optimised value obtained from the genetic algorithm) on the zero dispersion wavelength (ZWD) and nonlinear coefficient at 1550 nm. In all cases, when one parameter is varied the others are held constant.

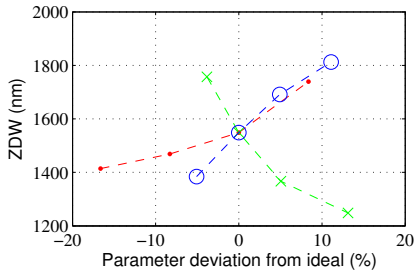

(a) Dispersion

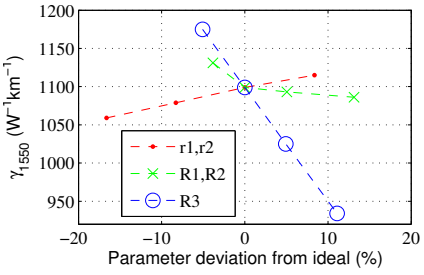

(b) Nonlinearity

Fig. 2: The effect of varying individual parameters on dispersion and nonlinearity

We see that as the size of the inner holes (r1, r2) decreases,

the ZDW moves to shorter wavelengths while the nonlinear coefficient gets smaller; as the radial distance of the holes from the center of the fiber (R1,R2) increases, the ZDW moves to shorter wavelengths while γ gets smaller ; as the core diameter (R3) increases, the ZDW moves to longer wavelengths while γ again gets smaller. We also see that, as expected, the sensitivity to r1, r2 is noticeably smaller since these parameters are of subwavelength dimensions.

In our genetic algorithm we have used a fitness function defined as in Eq. (9). Where $\gamma_{s,i}$ is the nonlinear coefficient at the signal/idler wavelength and D_j are the group velocity dispersions for a set of wavelengths, λ_j, in the band of interest.

$$F = \frac{\gamma_{s,i}}{\sum_j |D_j|} \tag{9}$$

This function serves as a figure of merit when evaluating the goodness of a particular set of input parameters within a 'population' of input parameter sets. Its physical significance is that it highlights those members (where each member is a set of input parameters) of the population that have high nonlinearity and low dispersion in the band of interest. The search heuristic then considers multiple sets of parameters (each being a candidate solution to the optimisation problem) as individuals in a population of solutions and evolves them towards better solutions, based on their fitness [22]. This type of evolutionary algorithm is routinely used in optimisation problems and has been used before for dispersion tailoring of microstructured optical fibers [23].

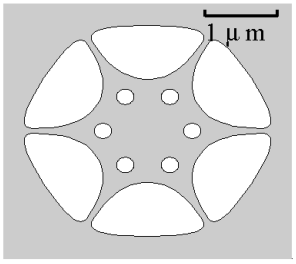

Fig. 3: Optimised fiber design (core region)

The final fiber design is shown in Fig. 3. This fiber has a group velocity dispersion $D = 0.14$ ps^{-1}nm^{-1}km^{-1} and nonlinear coefficient $\gamma = 1099$ W^{-1}km^{-1}, respectively at the telecoms wavelength of 1550 nm. Similar dispersion flattened nonlinear fibers have been fabricated recently [24], [25] showing the promise of highly nonlinear soft glass fiber designs for telecommunications applications [26], [27].

The power of this technique is seen by comparing the parametric gain g as a function of pump separation for the dispersion engineered MOF designed here with other highly nonlinear fibers. In Fig. 5 below we have looked at the gain for four types of fiber: (a) commercially available silica HNLF with flattened dispersion and ZDW at 1550 nm; (b), (c) two types of Bismuth-air step index fiber; and (d) the dispersion engineered fiber we have described above. In (b) the core diameter has been set to 3.6 μm so that the zero dispersion

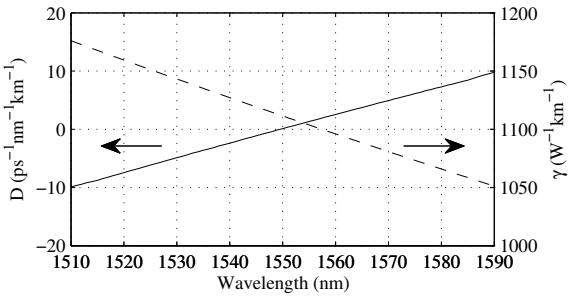

Fig. 4: Modelled dispersion and nonlinearity

wavelength is at 1550 nm (the same as the designed MOF). The fiber in (c) is exactly the same as (b), but for its nonlinear coefficient which has been artificially raised to match that of the designed MOF.

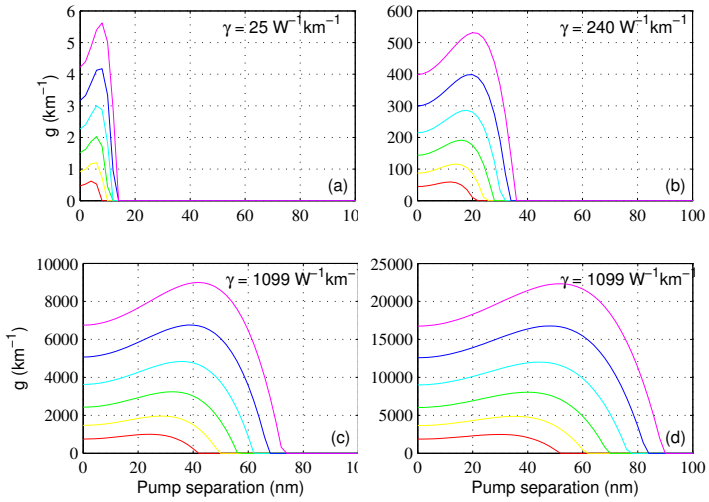

Fig. 5: Gain bandwidth for dispersion engineered fiber MOF compared to other highly nonlinear fibers. In the figures above P represents the power in either pump and the gain is defined as in Eq. (7). In all plots the ZDW is at 1550 nm.

For similar values of pump power, the gain per length gets successively higher and broader as we move from the silica fiber to the soft glass fibers, with the best performance being that of the dispersion engineered HWW fiber. By just maintaining the ZDW and increasing the γ value through the use of a material with a higher intrinsic nonlinearity the gain, per length, in (b) is already orders of magnitude higher and covers a broader band, relative to that in (a). The best gain has been achieved by combining dispersion flattening with high nonlinearity through the use of microstructure - as we have done with our optimised MOF. The gain in this case [i.e. (d)] is even significantly better that in (c) where we have artificially increased the nonlinear coefficient of the Bismuth-air step index fiber. This highlights the benefits of using soft glass based designs, both in terms of high material nonlinearity and the ability to specifically tailor and optimise the dispersion profile through the use of microstructure.

To achieve similar gain in a conventional silica HNLF one would require significantly higher pump powers or longer lengths, compared to the dispersion tailored, soft glass MOF. Generally, if the total power into the fiber is to be kept at a few Watts the required length of silica HNLF is of the order of a few 100 metres. In addition to this, the operating bandwidth, which is determined by the pump separation, of a Silica based HNLF is lower, irrespective of length. This is due to the fact that the region over which g is nonzero and real is narrower, as seen in Fig. 5.

IV. Modelling overview

Next, the performance of the designed MOF as a PSA device was analysed using a split-step Fourier pulse propagation model of the nonlinear Schrödinger equation (NLSE) [28], [29]. We use this numerical simulation method instead of the simplified coupled four wave equations as it allows us to more closely simulate real conditions. Pump depletion, for instance, and cascaded four wave mixing are not ignored and, as we show later, this allows us to consider the effect of saturation on the signal regeneration process.

The form of the NLSE in the time domain is shown in Eq. (10t), for a pulse with envelope A. Note that we have moved to the reference frame of the pulse where $T = t - z/v_g$.

$$\begin{aligned}\frac{\partial A}{\partial z} =& -\frac{\alpha}{2}A + \sum_{k\geqslant 2}\frac{i^{k+1}}{k}\beta_k\frac{\partial^k A}{\partial t^k} \\ &+ i\gamma\left[1 + i\tau_{shock}\frac{\partial}{\partial T}\right] \\ &\times\left[A\int R(T')|A(z,T-T')|^2 dT'\right] \end{aligned} \tag{10}$$

The first term on the right hand side includes the effect of loss thorough the absorption coefficient α; the second term gives us the effect of dispersion through β_k (the coefficients of the Taylor series expansion of the propagation constant $\beta(\omega)$ around the frequency ω_0); the third term handles all the nonlinear effects and includes the optical shock time, defined below [30].

$$\begin{aligned}\tau_{shock} =& \frac{1}{\omega_0} - \frac{1}{n_{eff}(\omega_0)}\frac{\partial n_{eff}(\omega)}{\partial\omega}\bigg|_{\omega_0} \\ &- \frac{1}{A_{eff}(\omega_0)}\frac{\partial A_{eff}(\omega)}{\partial\omega}\bigg|_{\omega_0}\end{aligned} \tag{11}$$

Where n_{eff} and A_{eff} are, respectively, the effective indices and effective areas of the propagating mode and ω_0 is the angular frequency about which the pulse is centred. The nonlinear response function $R(t)$ contained in Eq. (11) is given by [30].

$$R(t) = (1 - f_R)\delta(t) + f_(R)h_R(t) \tag{12}$$

The δ-function in the first term of Eq. (12) represents the instantaneous electronic response. This is responsible for all Kerr type effects such as self and cross phase modulation, along with four wave mixing. The second term represents the delayed Raman response of the ions in the glass. It is evaluated using the Raman fraction f_R and the Raman response function $h_R(t)$. For bismuth oxide glasses such as the one considered here the Raman gain may be evaluated using the Raman response function in [31] - where the Raman gain coefficient g_R/A_{eff}, as a function of frequency shift Δf, is shown to have two peaks of approximately 0.013 $\mathrm{W^{-1}m^{-1}}$ (at $\Delta f = 0.64$ THz) and 0.011 $\mathrm{W^{-1}m^{-1}}$ (at $\Delta f = 1.9$ THz); and goes to zero for frequency shifts larger than 3.2 THz.Thus, given the short fiber length, relatively low pump power and, most importantly, the fact that the pump-signal separation (29 nm = 3.7 THz) is larger than the Raman gain bandwidth of the first pump (at 1521 nm) we have not considered Raman effects in our simulations.

Additionally, It should be noted that since, as part of the split step method, the linear (dispersive) part of the equation is solved in the frequency domain through a $\beta(\omega)\tilde{A}(z,\omega)$ term the full effect of higher order dispersion is included in the simulation.

V. Simulation results

It is well known that by operating parametric amplifiers in the saturation regime one may limit or squeeze the amplitude of a train of input pulses. The signal gain is said to be saturated when the output power does not increase for further increases in the input signal power, past the saturation point. This happens mainly due to depletion of the pump energy [32] and is a useful mechanism for suppressing amplitude fluctuations.

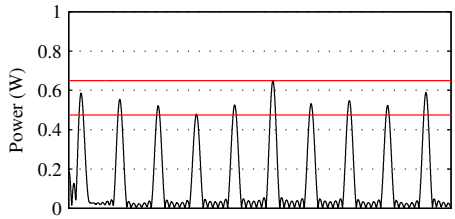

(a) Input signal

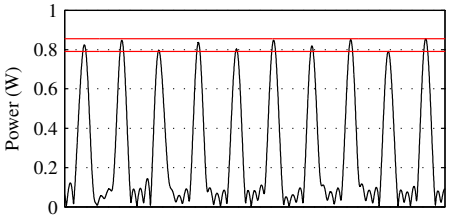

(b) Output

Fig. 6: Simultaneous reduction in amplitude noise ripple and amplification for a train of 640 Gb/s pulses

The noise suppression effect of operating in the gain saturation regime was first studied in semiconductor optical amplifiers (SOAs) [33], [34] before being demonstrated in fiber parametric optical amplifiers (FOPAs) [35]. Since four wave mixing based amplification also preserves phase, gain saturation is particularly useful for performance improvement

of DPSK signals [36], [37] as it counteracts the phase-to-amplitude noise conversion aspect of the transfer function.

The effect of saturation is seen in Fig. 6 where we see good power equalisation of the output pulses. For the input, we defined a train of 640 Gb/s pulses with equal pulse width and pulse separation of 78.1 ps. The simulated pump power and fiber length were 0.8 W (in each pump) and 53 cm, respectively. The fiber loss was set to be 2 dB/m.

We may quantify this by defining a ripple factor in the amplitude noise as $P_r = \Delta P/P_{RMS}$, where ΔP is the difference in power between the lowest and highest signals and P_{RMS} is the root mean square power. We then see that the amplitude noise ripple is reduced by 7.9 dB while the RMS power is amplified by 2.6 dB.

In order to achieve phase squeezing we have considered a four wave mixing scheme similar to [11], where the signal and idler are degenerate at 1550 nm and the two pumps are placed symmetrically apart (in frequency) such that the pump wavelengths are $\lambda_{P1} = 1521.1$ nm and $\lambda_{P2} = 1580.0$ nm. By having such a large pump to pump separation we minimise interactions between the two pumps and allow for high bandwidth signals. The fiber loss was again set to be 2 dB/m. We then ran the model on a train of noisy 640 Gb/s DPSK type input pulses which were defined, as earlier, to have equal width and separation of 78.1 ps. Noise was introduced into both the phase and the amplitude through a random number generator such that we would have a scatter of points, on a polar plot, similar to those obtained after transmission of DPSK pulses in a real system.

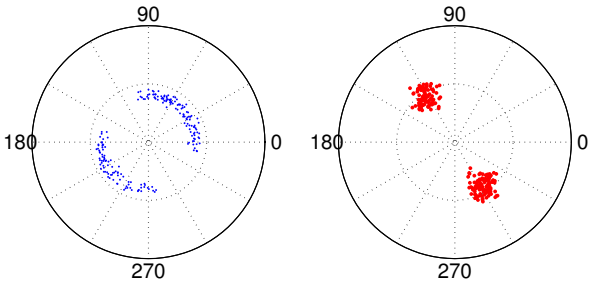

Fig. 7: Squeezing performance for 640 Gb/s pulses. The fiber length $l = 5$ m, pump powers $P_{\omega_{P1}} = P_{\omega_{P2}} = 0.8$ W and signal power $P_{\omega_s} = 0.35$ W

The results, seen in Fig. 7, show squeezing of over 90° phase noise to just over 20° without a significant penalty in amplitude noise. This level of squeezing is comparable to what has currently been achieved experimentally at bit rates of 40 Gb/s, but is demonstrated here for an ultrafast, broadband input signal at 640 Gb/s. Note that the rotation in absolute phase of the signals due to the buildup of linear phase as the pulses propagate down the fiber is not important for differentially encoded formats like DPSK. In any case, the absolute phase can be rotated by changing the pump phases appropriately.

VI. Effect of structural deviations in fiber design on PSA performance

By designing a MOF to have high gain within relatively short lengths it can tolerate both the effect of variations in the zero dispersion wavelength due to structural fluctuations along the fiber length and the inevitable deviations from the ideal structure that happen during fabrication.

Fig. 8 shows the variations in fiber dispersion and nonlinearity for deviations from the ideal structure. These structures have been numerically altered from the ideal case by uniformly stretching/contracting the fiber parameters by -10%, +10% and +20%, relative to the the ideal case (the ideal structure has also been included for comparison). Fabrication of fibers similar to the one that has been designed here indicate that fabrication distortion does indeed lead to a final structure where the key structural parameters are scaled by approximately 10%, relative to the ideal design [25].

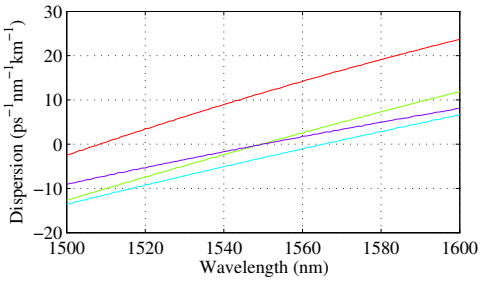

(a) Dispersion

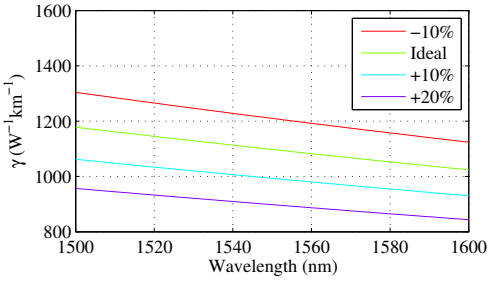

(b) Nonlinearity

Fig. 8: The effect, on dispersion and nonlinearity, of scaling the fiber design.

The most significant change is seen in the -10% case where the zero dispersion wavelength moves to a much shorter wavelength, relative to the ideal case. For the other cases we notice much less fluctuation in the dispersion. The change in the nonlinearity is as expected - as the structure gets smaller γ increases due to the mode being more confined, while an increase in size leads to less confinement and a lower γ.

As dispersion and nonlinearity curves by themselves don't paint the entire picture of PSA we have also looked at the phase responses for these structures - shown in Fig. 9. The phase response here is defined as the gain of the input signal as a function of its initial phase. As is typical for phase sensitive amplification, the phase responses show the gain periodically oscillating with phase where the input signal phases for which

the gain is highest are separated from those for which the gain is lowest by $\pi/2$. Ideally, one would want this gain discrimination to be as large as possible as it determines how 'tightly' the phase noise is squeezed.

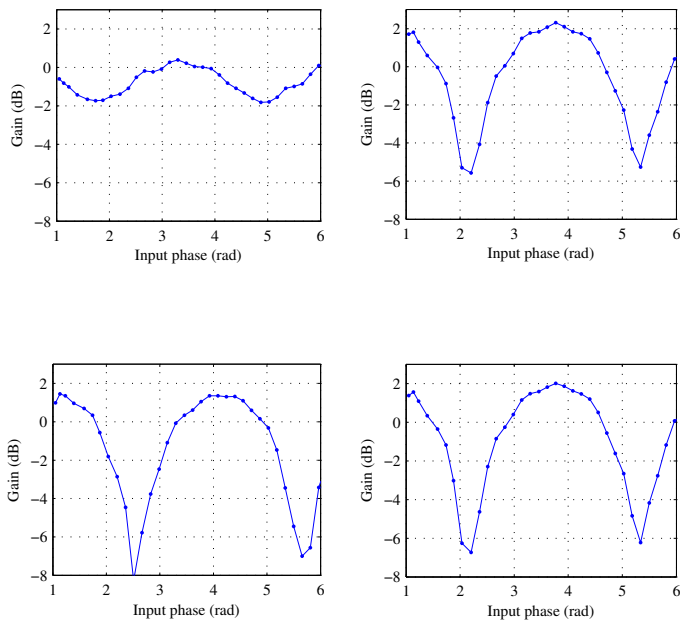

Fig. 9: Phase response for deviations from the ideal fiber structure: ideal structure -10% (top left), ideal structure (top right), ideal structure +10% (bottom left), ideal structure +20% (bottom right)

We see that as the performance of the fiber design suffers considerably for a change in the structure of -10%. However, the results also show that the fiber performance in the 100% to 120% range is quite similar. In some instances, such as for the +10% case, the squeezing is slightly improved, albeit with less amplitude gain. Given this tradeoff we believe the ideal design is still the best case. However the similar performance shown in (b), (c) and (d) indicate that the high nonlinearity of this fiber allows us to tolerate fluctuations in the dispersion at the signal wavelength quite well, provided it remains sufficiently small and normal.

This indicates that we are able to get good fabrication tolerance by aiming for a structure that is slightly larger than the optimal design. Note that, for comparison, these simulations were all done with the same values of pump and signal power and phase. By optimising these parameters one may improve the performance of a non ideal structure even further, to bring it closer to the response of the ideal fiber.

VII. Conclusion

We have designed an optical fiber using a genetic algorithm based technique to have low dispersion and high nonlinearity at the telecoms wavelength of 1550 nm. Its performance has been simulated numerically using a split-step Fourier analysis of the NLSE, indicating that this fiber could be used to perform broadband phase sensitive amplification for high speed telecommunication networks, operating at speeds up to 640 Gb/s. The fiber design has a high gain and short operating length. Analysis of performance when subjected to structural variations that are expected during fabrication show that we are able to compensate against such changes in the dispersion profile, mostly due to the high nonlinearity.

It is worth highlighting the fact that the fiber length used in these simulations is only 5 m, which is two orders of magnitude lower than the lengths generally used in silica HNLF based PSA devices. This is not only useful for building compact devices but may be used to simultaneously perform phase and amplitude amplification without the need to suppress the Stimulated Brillouin Scattering (SBS). Although this will need to be investigated experimentally once the fiber is fabricated, the Brillouin coefficient for Bismuth oxide based nonlinear fibers has been shown to be an order of magnitude less than a silica based HNLF [38].

Further work will focus on fiber fabrication and device integration.

VIII. Acknowledgements

The authors would like to thank David Richardson at the Optoelectronics Research Centre, University of Southampton for his valuable insight and discussions on the material presented herein. We would also like to acknowledge ARC funding support (DP110104247). Tanya M. Monro acknowledges the support of an ARC Federation Fellowship.

References

[1] D. Walls, "Squeezed states of light," *Nature*, vol. 306, pp. 141–146, 1983.

[2] H. Yuen, "Two-photon coherent states of the radiation field," *Physical Review A*, vol. 13, no. 6, p. 2226, 1976.

[3] A. Gnauck and P. Winzer, "Optical phase-shift-keyed transmission," *Lightwave Technology, Journal of*, vol. 23, no. 1, pp. 115–130, 2005.

[4] M. Rohde, C. Caspar, N. Heimes, M. Konitzer, E. Bachus, and N. Hanik, "Robustness of dpsk direct detection transmission format in standard fibre wdm systems," *Electronics Letters*, vol. 36, no. 17, pp. 1483–1484, 2000.

[5] H. Haus and J. Mullen, "Quantum noise in linear amplifiers," *Physical Review*, vol. 128, no. 5, pp. 2407–2413, 1962.

[6] A. Bogris, D. Syvridis, and C. Efstathiou, "Noise Properties of Degenerate Dual Pump Phase Sensitive Amplifiers," *Lightwave Technology, Journal of*, vol. 28, no. 8, pp. 1209–1217, 2010.

[7] Z. Tong, C. Lundström, P. Andrekson, C. McKinstrie, M. Karlsson, D. Blessing, E. Tipsuwannakul, B. Puttnam, H. Toda, and L. Grüner-Nielsen, "Towards ultrasensitive optical links enabled by low-noise phase-sensitive amplifiers," *Nature Photonics*, vol. 5, no. 7, pp. 430–436, 2011.

[8] K. Croussore, C. Kim, and G. Li, "All-optical regeneration of differential phase-shift keying signals based on phase-sensitive amplification," *Optics letters*, vol. 29, no. 20, pp. 2357–2359, 2004.

[9] K. Croussore, I. Kim, C. Kim, Y. Han, and G. Li, "Phase-and-amplitude regeneration of differential phase-shift keyed signals using a phase-sensitive amplifier," *Optics Express*, vol. 14, no. 6, pp. 2085–2094, 2006.

[10] R. Slavík, F. Parmigiani, J. Kakande, C. Lundström, M. Sjödin, P. Andrekson, R. Weerasuriya, S. Sygletos, A. Ellis, L. Grüner-Nielsen *et al.*, "All-optical phase and amplitude regenerator for next-generation telecommunications systems," *Nature Photonics*, 2010.

[11] J. Kakande, C. Lundström, P. Andrekson, Z. Tong, M. Karlsson, P. Petropoulos, F. Parmigiani, and D. Richardson, "Detailed characterization of a fiber-optic parametric amplifier in phase-sensitive and phase-insensitive operation," *Optics Express*, vol. 18, no. 5, pp. 4130–4137, 2010.

[12] J. Schröder, T. Vo, Y. Paquot, and B. Eggleton, "Breaking the tbit/s barrier: Higher bandwidth optical processing," *Optics and Photonics News*, vol. 23, no. 3, pp. 32–37, 2012.

[13] C. McKinstrie and S. Radic, "Phase-sensitive amplification in a fiber," *Opt. Express*, vol. 12, no. 20, pp. 4973–4979, 2004. [Online]. Available: http://www.opticsexpress.org/abstract.cfm?URI=oe-12-20-4973

[14] C. Garrett and F. Robinson, "Miller's phenomenological rule for computing nonlinear susceptibilities," *Quantum Electronics, IEEE Journal of*, vol. 2, no. 8, pp. 328–329, 1966.

[15] H. Ebendorff-Heidepriem, P. Petropoulos, S. Asimakis, V. Finazzi, R. Moore, K. Frampton, F. Koizumi, D. Richardson, and T. Monro, "Bismuth glass holey fibers with high nonlinearity," *Opt. Express*, vol. 12, no. 21, pp. 5082–5087, Oct 2004. [Online]. Available: http://www.opticsexpress.org/abstract.cfm?URI=oe-12-21-5082

[16] D. Milam, "Review and assessment of measured values of the nonlinear refractive-index coefficient of fused silica," *Applied optics*, vol. 37, no. 3, pp. 546–550, 1998.

[17] H. Ebendorff-Heidepriem, P. Petropoulos, S. Asimakis, V. Finazzi, R. Moore, K. Frampton, F. Koizumi, D. Richardson, and T. Monro, "Bismuth glass holey fibers with high nonlinearity," *Optics Express*, vol. 12, no. 21, pp. 5082–5087, 2004.

[18] K. Kikuchi, K. Taira, and N. Sugimoto, "Highly-nonlinear bismuth oxide-based glass fibers for all-optical signal processing," in *Optical Fiber Communication Conference*. Optical Society of America, 2002.

[19] S. Afshar V, W. Zhang, H. Ebendorff-Heidepriem, and T. Monro, "Small core optical waveguides are more nonlinear than expected: experimental confirmation," *Optics letters*, vol. 34, no. 22, pp. 3577–3579, 2009.

[20] W. Q. Zhang, S. Afshar V., and T. M. Monro, "A genetic algorithm based approach to fiber design for high coherence and large bandwidth supercontinuum generation," *Opt. Express*, vol. 17, no. 21, pp. 19 311–19 327, Oct 2009. [Online]. Available: http://www.opticsexpress.org/abstract.cfm?URI=oe-17-21-19311

[21] W. Q. Zhang, J. E. Sharping, R. T. White, T. M. Monro, and S. Afshar V., "Design and optimization of fiber optical parametric oscillators for femtosecond pulse generation," *Opt. Express*, vol. 18, no. 16, pp. 17 294–17 305, Aug 2010. [Online]. Available: http://www.opticsexpress.org/abstract.cfm?URI=oe-18-16-17294

[22] L. Davis, *Handbook of genetic algorithms*. Van nostrand reinhold, 1991.

[23] F. Poletti, V. Finazzi, T. Monro, N. Broderick, V. Tse, and D. Richardson, "Inverse design and fabrication tolerances of ultra-flattened dispersion holey fibers," *Optics Express*, vol. 13, no. 10, pp. 3728–3736, 2005.

[24] F. Poletti, X. Feng, G. Ponzo, M. Petrovich, W. Loh, and D. Richardson, "All-solid highly nonlinear singlemode fibers with a tailored dispersion profile," *Optics Express*, vol. 19, no. 1, pp. 66–80, 2011.

[25] W. Q. Zhang, H. Ebendorff-Heidepriem, T. M. Monro, and S. Afshar V., "Fabrication and supercontinuum generation in dispersion flattened bismuth microstructured optical fiber," *Opt. Express*, vol. 19, no. 22, pp. 21 135–21 144, Oct 2011. [Online]. Available: http://www.opticsexpress.org/abstract.cfm?URI=oe-19-22-21135

[26] A. Camerlingo, F. Parmigiani, X. Feng, F. Poletti, P. Horak, W. Loh, D. Richardson, and P. Petropoulos, "Multichannel wavelength conversion of 40-gb/s nonreturn-to-zero dpsk signals in a lead–silicate fiber," *Photonics Technology Letters, IEEE*, vol. 22, no. 15, pp. 1153–1155, 2010.

[27] A. Camerlingo, F. Parmigiani, X. Feng, F. Poletti, P. Horak, W. Loh, D. Richardson, and P. Petropoulos, "Wavelength conversion in a short length of a solid lead–silicate fiber," *Photonics Technology Letters, IEEE*, vol. 22, no. 9, pp. 628–630, 2010.

[28] T. Taha and M. Ablowitz, "Analytical and numerical aspects of certain nonlinear evolution equations. ii. numerical, nonlinear schrödinger equation," *Journal of Computational Physics*, vol. 55, no. 2, pp. 203–230, 1984.

[29] O. Sinkin, R. Holzlöhner, J. Zweck, and C. Menyuk, "Optimization of the split-step fourier method in modeling optical-fiber communications systems," *Journal of lightwave technology*, vol. 21, no. 1, p. 61, 2003.

[30] G. Agrawal, *Nonlinear fiber optics*. Academic press, 2001.

[31] C. Cantini, K. Abedin, F. Saachi, G and. Pasquale, and F. Kubota, "Measurement of Raman Gain Coefficient in Bismuth-Based Single ModeOptical Fibres ", in *Tenth Optoelectronics and Communications Conference Technical digest*, 2005, pp. 234–235.

[32] K. Inoue, "Optical level equalisation based on gain saturation in fibre optical parametric amplifier," *Electronics Letters*, vol. 36, no. 12, pp. 1016–1017, 2000.

[33] M. Shtaif and G. Eisenstein, "Noise properties of nonlinear semiconductor optical amplifiers," *Optics letters*, vol. 21, no. 22, pp. 1851–1853, 1996.

[34] M. Shtaif and G. Eisenstein, "Experimental study of the statistical properties of nonlinearly amplified signals in semiconductor optical amplifiers," *Photonics Technology Letters, IEEE*, vol. 9, no. 7, pp. 904–906, 1997.

[35] K. Inoue and T. Mukai, "Experimental study on noise characteristics of a gain-saturated fiber optical parametric amplifier," *Journal of lightwave technology*, vol. 20, no. 6, p. 969, 2002.

[36] M. Matsumoto and K. Sanuki, "Performance improvement of dpsk signal transmission by a phase-preserving amplitude limiter," *Optics Express*, vol. 15, no. 13, pp. 8094–8103, 2007.

[37] J. Hansryd, P. Andrekson, M. Westlund, J. Li, and P. Hedekvist, "Fiber-based optical parametric amplifiers and their applications," *Selected Topics in Quantum Electronics, IEEE Journal of*, vol. 8, no. 3, pp. 506–520, 2002.

[38] J. Lee, T. Nagashima, T. Hasegawa, S. Ohara, N. Sugimoto, and K. Kikuchi, "Bismuth-oxide-based nonlinear fiber with a high sbs threshold and its application to four-wave-mixing wavelength conversion using a pure continuous-wave pump," *Journal of lightwave technology*, vol. 24, no. 1, p. 22, 2006.